

# GEOMETRICALLY AND PHYSICALLY NON-LINEAR MODELS FOR SOFT TISSUE SIMULATION

J.-M. Schwartz<sup>1</sup>, D. Laurendeau<sup>2</sup>, M. Denninger<sup>3</sup> and D. Rancourt<sup>4</sup>

## 1. ABSTRACT

We describe extensions of the tensor-mass algorithm allowing fast computation of non-linear and visco-elastic mechanical forces and deformations for the simulation of biological soft tissue. This work is part of a broader project aiming at the development of a simulation tool for the planning of cryogenic surgical treatment of liver cancer. Real-time deformation algorithms are usually based on linear elasticity, but the simulation of percutaneous surgery requires more accurate modelling of soft tissue. Two types of non-linear extensions of the tensor-mass model are discussed here: a *physically non-linear* model, involving non-linear stress-strain relationships, and a *geometrically non-linear* or *large displacement* model. Both simulation models are compared to experimental data obtained under perforation of a deer liver sample by a biopsy needle.

## 2. INTRODUCTION

The first algorithms for fast computation of mechanical forces and deformations made use of the linear elastic mechanical model [1, 2, 3]. Bro-Nielsen and Cotin showed that Finite Element Methods could be used for real-time applications, first with a quasi-static formulation [4], and later with a dynamical formulation called the *tensor-mass* model [5]. However, experimental characterizations revealed that linear elasticity is only a coarse approximation of the real properties of biological soft tissues. For example a thorough study of the mechanical properties of swine brain tissue conducted by Miller and Chinzei [6] showed that brain tissue was highly non-linear, and that a visco-elastic constitutive model was most suitable for modelling brain tissue deformations. Similar conclusions were reached by Farshad *et al.* [7] from experiments on the swine kidney.

For this reason, we aimed at designing an algorithm allowing real-time computation of non-linear visco-elastic behaviours. Zhuang and Canny [8] developed a fast finite element based method that integrates geometrical non-linearity. In a similar approach Wu *et al.* [9] additionally integrated physical non-linearity for hyper-elastic materials. Picinbono *et al.* [10] developed an extension of the tensor-mass algorithm integrating geometrical non-linearity. An important quality of the tensor-mass model is to allow real-time topology changes in the finite element mesh, which is a requirement for the simulation of most if not all surgical applications.

Keywords: surgery simulation, soft tissue, non-linear model, deformations, forces

---

<sup>1</sup> Ph.D. Student, Computer Vision and Systems Laboratory, Laval University, Québec (Qc) G1K 7P4, Canada

<sup>2</sup> Professor, Computer Vision and Systems Laboratory, Laval University, Québec (Qc) G1K 7P4, Canada

<sup>3</sup> M.D. Student, Biomechanics Laboratory, Laval University, Québec (Qc) G1K 7P4, Canada

<sup>4</sup> Professor, Biomechanics Laboratory, Laval University, Québec (Qc) G1K 7P4, Canada

### 3. THE LINEAR ELASTIC TENSOR-MASS MODEL

In the tensor-mass algorithm, the modelled object is discretized into a conformal tetrahedral mesh as defined by finite element theory. Inside every tetrahedron  $T_l$ , the displacement field is defined by linear interpolation of the displacement vectors of the four vertices of  $T_l$ . The linear elastic energy of tetrahedron  $T_l$  can then be expressed as a function of the displacements of the four vertices and of the two Lamé coefficients of the material,  $\lambda$  and  $\mu$ . The force vector  $\mathbf{f}_{T_l(j)}$  applied to vertex  $j$  of tetrahedron  $T_l$  is defined as the derivate of the elastic energy and expressed by

$$\mathbf{f}_{T_l(j)} = \sum_{k=0}^3 \mathbf{K}_{jk}^{T_l} \mathbf{u}_{T_l(k)} \quad (1)$$

where  $\mathbf{u}_{T_l(k)}$  is the displacement of vertex  $k$  of tetrahedron  $T_l$  with regard to its rest position, and  $\mathbf{K}_{jk}^{T_l}$  are stiffness tensors of size  $3 \times 3$  that depend only on the rest geometry of  $T_l$  and on the Lamé coefficients. The detailed expression of tensors  $\mathbf{K}_{jk}^{T_l}$  has been provided by Cotin *et al.* [5]. These tensors can be pre-computed, therefore real-time computation is restricted to a combination of matrix-vector multiplications and matrix summations.

Given a complete mesh, the total elastic force  $\mathbf{f}_i$  applied onto every vertex  $i$  is obtained by summing the forces contributed by all adjacent tetrahedrons of  $i$ . The resulting system is solved dynamically, the motion of every vertex is determined by a Newtonian equation which takes the form

$$m_i \ddot{\mathbf{u}}_i + \gamma_i \dot{\mathbf{u}}_i - \mathbf{f}_i = 0 \quad (2)$$

where  $m_i$  and  $\gamma_i$  are respectively the mass and the damping coefficient associated to vertex  $i$ . Mass and damping effects are supposed to be lumped at vertices.

### 4. MODEL EXTENSIONS

In the classical definition of linear elasticity, linearity is assumed at two different levels. First, quadratic terms are eliminated from the strain tensor, implying that small deformations are assumed, this hypothesis may be called *geometrical linearity*. Second, the relation between the stress and strain tensors is assumed to be linear, this hypothesis may be called *physical linearity*.

#### 4.1 Adding physical non-linearity

In expression (1), the force field inside a tetrahedron is expressed as a linear combination of the displacements of the four tetrahedron vertices. Physical non-linearity can be simulated by dynamically and locally modifying the stiffness tensors, depending on the local deformation conditions, thus avoiding restriction to a particular class of mechanical models. Stiffness tensors cannot be modified arbitrarily as the isotropy properties of the material must be satisfied. When all possible space symmetries have been considered, only two degrees of freedom remain for an isotropic material, corresponding to the two Lamé coefficients. Therefore acting on the Lamé coefficients themselves is an easy way to modify the local elastic properties of the material in real-time, while satisfying isotropy constraints and covering the complete space of possible isotropic behaviours.

Stiffness tensors  $\mathbf{K}_{jk}^{T_l}$  can be divided into two components proportional to  $\lambda$  and  $\mu$

$$\mathbf{K}_{jk}^{T_l} = \lambda \mathbf{A}_{jk}^{T_l} + \mu \mathbf{B}_{jk}^{T_l} \quad (3)$$

where tensors  $\mathbf{A}_{jk}^{T_l}$  and  $\mathbf{B}_{jk}^{T_l}$  share the same properties as  $\mathbf{K}_{jk}^{T_l}$  and can still be pre-computed. Then a non-linear expression can be computed under the form

$$\mathbf{f}_{T_l(j)} = \sum_{k=0}^3 \left( \mathbf{K}_{jk}^{T_l} + \delta\lambda(T_l) \mathbf{A}_{jk}^{T_l} + \delta\mu(T_l) \mathbf{B}_{jk}^{T_l} \right) \mathbf{u}_{T_l(k)} \quad (4)$$

where  $\delta\lambda(T_l)$  and  $\delta\mu(T_l)$  are non-linear corrective functions.  $\delta\lambda$  and  $\delta\mu$  depend on the local deformation of the mesh element  $T_l$ . The choice for their expression as a function of the shape of a tetrahedron determines the type of non-linear law being simulated.

A quantification of the local mesh element deformation has to be used as an argument for  $\delta\lambda$  and  $\delta\mu$ . Different measures may be considered, including strain tensor invariants or tetrahedron shape measures. Because of the empirical nature of the method, the choice of a particular measure does not significantly affect the overall behaviour of the system. In this study, the *tetrahedron mean ratio* as defined by Liu and Joe [11] was used, mainly for computational speed concerns. Examples of possible behaviours that can be simulated using this technique have been described previously [12].

#### 4.2 Adding geometrical non-linearity

Picinbono *et al.* [10] introduced an extension of the tensor-mass algorithm that uses a non-linear Cauchy-Green strain tensor, while keeping physical linearity. The properties and overall structure of the algorithm remain unchanged, but the extension results in a number of additional terms in the expression of force  $\mathbf{f}_i$

$$\mathbf{f}_{T_l(j)} = \sum_{k=0}^3 \mathbf{K}_{jk}^{T_l} \mathbf{u}_k + \sum_{k,m=0}^3 (\mathbf{u}_m \mathbf{u}_k^T) \mathbf{c}_{kmj}^{T_l} + \frac{1}{2} (\mathbf{u}_k \cdot \mathbf{u}_m) \mathbf{c}_{jkm}^{T_l} + 2 \sum_{k,m,n=0}^3 d_{kmnj}^{T_l} \mathbf{u}_n \mathbf{u}_m^T \mathbf{u}_k \quad (5)$$

where  $\mathbf{K}_{jk}^{T_l}$  are the stiffness tensors described in Section 3,  $\mathbf{c}_{jkm}^{T_l}$  are vectors and  $d_{jkmn}^{T_l}$  are scalars. All these parameters can be pre-computed as with the stiffness tensors.

A comparison between the linear model and the geometrically non-linear model in a simulation of compression of a three-dimensional model mesh is shown in Figure 1. As could be expected, the two models lie very close when deformations remain small, but differences arise and become overwhelming when deformations get larger.

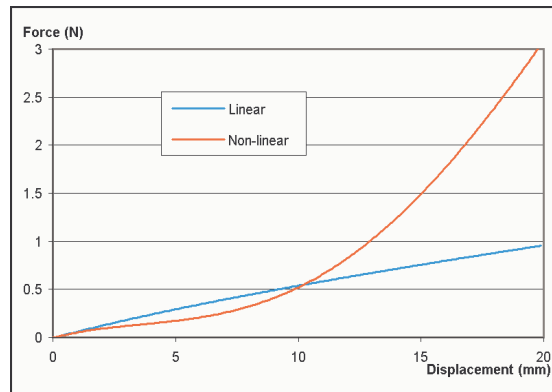


Figure 1. Forces in the simulated compression of a three-dimensional mesh computed by a linear elastic (blue) and a geometrically non-linear (red) tensor-mass model.

The geometrically and physically non-linear models can easily be combined. Figure 2 compares the deformations observed in the compression of a three-dimensional model mesh for a physically non-linear model only (a) and for the combination of both models (b). Sensible differences can be noticed between the two deformed states, in particular for the mesh elements surrounding the compression hole. The linear model is known to produce shape distortions in cases where a part of an object undergoes a rotation [10], which is typically the case for these elements. The Cauchy-Green based model conserves surface shapes more truthfully and produces a more realistic behaviour.

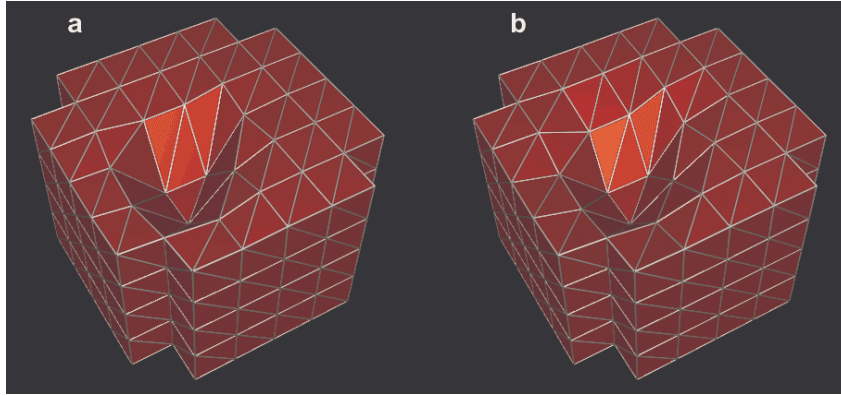


Figure 2. Deformation state of two models after compression has been applied onto one face of the top during 1.5 s with a velocity of 10 mm/s. a) Physically non-linear model only. b) Combination of physically and geometrically non-linear models.

#### 4.3 Adding visco-elasticity

Visco-elasticity can be introduced into the tensor-mass model provided that viscous modelling be restricted to a simple linear relation. We introduced a viscous force that is proportional to the speed of deformation and to a viscosity coefficient  $\eta$ . The obtained expression for the force is

$$\mathbf{f}_{T_i(j)}^{(v)} = \sum_{k=0}^3 \mathbf{K}_{jk}^{T_i} \dot{\mathbf{u}}_{T_i(k)} \quad (6)$$

where  $\mathbf{K}_{jk}^{T_i}$  are  $3 \times 3$  tensors depending only on the rest geometry of tetrahedron  $T_i$  and on the viscosity coefficient  $\eta$ , that still can be pre-computed.

The resulting visco-elastic model is a Voigt-Kelvin one, which does only provide approximate modelling of the properties of soft tissue. But when high computational speed is a top priority, this model is the very simplest that can be introduced into the tensor-mass framework. Integration of more advanced visco-elastic models appears to be more challenging and computationally expensive.

## 5. EXPERIMENTAL VALIDATION

Experimental measurements were conducted to assess the suitability of these models to the simulation of biological soft tissue. A 2.4 mm diameter biopsy needle was mounted on a 5 lbs Totalcomp TMB-5 load cell. The needle could be moved vertically by a step-motor whose velocity ranged from 2 to 10 mm/s. It was used to perforate a sample of deer liver placed in a container. The force modulus exerted onto the needle was

acquired together with its position at a rate of 500 Hz by an A/D sampling board.

Results showed to be highly reproducible. For a given velocity, all force curves were very similar, independently of the position where the sample was reached or of the orientation of the sample. The point where membrane rupture occurred was variable, but this variability could not be linked to the behaviour before rupture.

Both models, whether geometrical non-linearity was included or not, were successfully able to reproduce experimental data for the different velocities that were tested (Figure 3). Numerical values to be used for the  $\delta\lambda$  and  $\delta\mu$  functions are lower for the geometrically non-linear model, since it produces a sharper growth in force by itself.

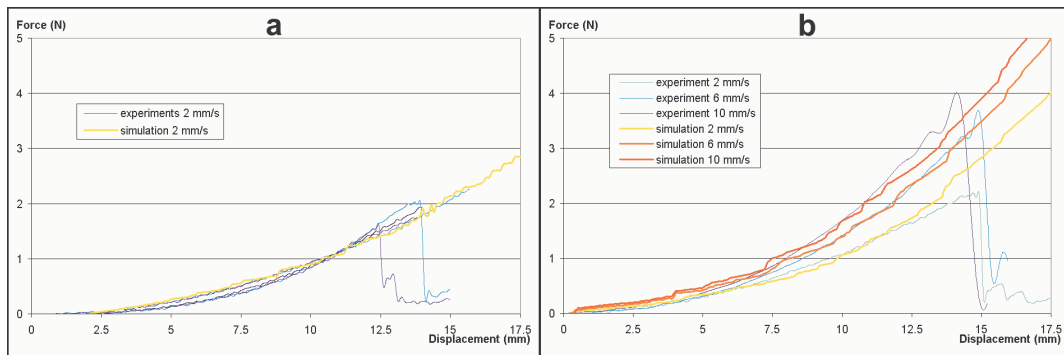


Figure 3: Experimentally measured forces in the perforation of liver tissue by a biopsy needle compared to simulations. a) Five experimental curves measured for a needle speed of 2 mm/s, and simulated force by the physically non-linear model. b) Three experimental curves measured for different needle speeds, and the corresponding simulated forces by the physically and geometrically non-linear model.

## 6. COMPUTATIONAL SPEED

Computational time required by these algorithms increases linearly with the number of mesh elements. The physically non-linear model needs 7-fold more time than the linear elastic model, and addition of geometrical non-linearity increases time by another factor 7. On a 1 GHz Pentium III processor, an iteration rate of 50 Hz could be achieved with meshes of up to 17000 tetrahedrons for the linear elastic model, 2500 tetrahedrons for the physically non-linear algorithm, and 350 tetrahedrons for the full algorithm.

Efficiency of the non-linear algorithms can be improved by making use of a non-linearity threshold. In typical applications, high deformations are limited to small areas of the mesh while most mesh elements are only slightly deformed. The linear model is sufficient for small deformations, so by leaving aside the non-linear terms for elements whose deformation is smaller than a given threshold value, the computational load can be focused onto the limited number of mesh elements that bring the key contribution.

## 7. DISCUSSION AND CONCLUSION

The main drawback of the full non-linear tensor-mass model lies in its low computational speed. In the present state, performance is not good enough to allow its

use in real-time on realistic models of biological organs. Yet, the physically non-linear model alone is fast enough for real-time applications, and its modelling accuracy cannot be distinguished from the full model in our experiments. For this reason it provides an interesting solution for simulation of biological soft tissue.

Additional experimental characterizations would definitely be useful to fully validate this model and to assess to degree of approximation involved by geometrical linearization. Measurements of three-dimensional deformations of biological samples would allow to distinguish the accuracy of both models, and remains a goal for the future. In addition, *in vivo* mechanical data of liver tissue will be necessary to build an accurate mechanical model of liver suitable for surgery simulation, as differences between the properties of living and dead biological tissue are significant.

## 8. REFERENCES

- [1] Cover, S. A., Ezquerra, N. F., O'Brien, J. F., Rowe, R., Gadacz, T., Palm, E., Interactively deformable models for surgery simulation, IEEE Computer Graphics and Applications, 1993, Vol. 13(6), 68-75.
- [2] Kühnapfel, U., Kuhn, C., Hübner, M., Krumm, H.-G., Maaß, H., Neisius, B., The Karlsruhe endoscopic surgery trainer as an example for virtual reality in medical education, Minimally Invasive Therapy & Allied Technologies, 1997, Vol. 6, 122-125.
- [3] James, D. L., Pai, D. K., Accurate real-time deformable objects, Proc. SIGGRAPH '99, 65-72.
- [4] Bro-Nielsen, M., Finite element modeling in surgery simulation, Proceedings of the IEEE, 1998, Vol. 86(3), 490-503.
- [5] Cotin, S., Delingette, H., Ayache, N., A hybrid elastic model for real-time cutting, deformations, and force feedback for surgery training and simulation, Visual Computer, 2000, Vol. 16(8), 437-452.
- [6] Miller, K., Chinzei, K., Constitutive modelling of brain tissue: experiment and theory, Journal of Biomechanics, 1997, Vol. 30(11/12), 1115-1121.
- [7] Farshad, M., Barbezat, M., Flüeler, P., Schmidlin, F., Graber, P., Niederer, P., Material characterization of the pig kidney in relation with the biomechanical analysis of renal trauma, Journal of Biomechanics, 1999, Vol. 32(4), 417-425.
- [8] Zhuang, Y., Canny, J., Haptic interactions with global deformations, Proc. ICRA 2000, Vol. 3, 2428-2433.
- [9] Wu, X., Downes, M. C., Goktekin, T., Tendick, F., Adaptive nonlinear finite elements for deformable body simulation using dynamic progressive meshes, Proc. Eurographics 2001, 349-358.
- [10] Picinbono, G., Delingette, H., Ayache, N., Non-linear anisotropic elasticity for real-time surgery simulation, Graphical Models, 2003, Vol. 65(5), 305-321.
- [11] Liu, A., Joe, B., Relationship between tetrahedron shape measures, BIT, 1994, Vol. 34(2), 268-287.
- [12] Schwartz, J.-M., Denninger, M., Rancourt, D., Moisan, C., Laurendeau, D., Modelling liver tissue properties using a non-linear visco-elastic model for surgery simulation. MS4CMS '02, ESAIM Proceedings, Vol. 12, 146-153.